

59-34
4972

**Baseline Experimental Investigation of an Electrohydrodynamically
Assisted Heat Pipe**

Final Report
1994 NASA/ASEE Summer Faculty Fellowship Program
Johnson Space Center

Submitted by:
A. B. Duncan¹

Assistant Professor
University of Illinois at Chicago

NASA/JSC

Directorate: Engineering

Division: Crew and Thermal Systems


Branch: Thermal Systems

JSC Colleague: Kathryn Miller Hurlbert

Date Submitted: August 4, 1994

Contract Number: NGT-44-005-803


Kathryn Miller Hurlbert


Allen B. Duncan

¹Direct All Correspondence to:
Dr. A. B. Duncan
Department of Mechanical Engineering (M/C 251)
University of Illinois at Chicago
Engineering Research Facility
842 W. Taylor St.
Chicago, IL 60607-7022

REFERENCES

1. F. Horz, M. Cintala, R. Bernhard and T. See, Dimensionally Scaled Penetration Experiments: Aluminium targets and glass projectiles 50 μm to 3.2 mm in diameter. *Int. J. Impact Engng* Vol. 15, No. 3, pp. 257-280 (1994).
2. A. J. Stilp, V. Hohler, E. Schneider and K. Weber, Debris cloud expansion studies. *Int. J. Impact Engng* 10, 543-559 (1990).
3. A. J. Pietkutowsky, A simple dynamic model for the formation of debris cloud. *Int. J. Impact Engng* 10, 453-472 (1990).
4. X. Weng and C. H. Yew, Hypervelocity impact of two sphere. *Int. J. Impact Engng* 8, 229-240 (1989).
5. D. E. Grady and S. L. Passmann, stability and fragmentation of ejecta in hypervelocity impact. *Int. J. Impact Engng* 10, 197-212 (1989).
6. R. J. Lawrence, A simple model for the optimization of stand-off hypervelocity particle shields. *Int. J. Impact Engng*. Vol. 5, pp. 451-461 (1987).
7. A. Watts, D. Atkinson and S. Rieco, Dimensional scaling for impact cratering and perforation. NASA contractor report, NCR 188259, March 16, 1993.

ABSTRACT

The increases in power demand and associated thermal management requirements of future space programs such as potential Lunar/Mars missions will require enhancing the operating efficiencies of thermal management devices. Currently, the use of electrohydrodynamically (EHD) assisted thermal control devices is under consideration as a potential method of increasing thermal management system capacity. The objectives of the currently described investigation included completing build-up of the EHD-Assisted Heat Pipe Test bed, developing test procedures for an experimental evaluation of the unassisted heat pipe, developing an analytical model capable of predicting the performance limits of the unassisted heat pipe, and obtaining experimental data which would define the performance characteristics of the unassisted heat pipe.

The information obtained in the currently proposed study will be used in order to provide extensive comparisons with the EHD-assisted performance observations to be obtained during the continuing investigation of EHD-Assisted heat transfer devices. Through comparisons of the baseline test bed data and the EHD assisted test bed data, accurate insight into the performance enhancing characteristics of EHD augmentation may be obtained. This may lead to optimization, development, and implementation of EHD technology for future space programs.

INTRODUCTION

The power demand and thermal management requirements of future space programs will require improving the efficiencies of thermal management devices. Currently, electrohydrodynamically assisted heat pipes are being considered for implementation in spacecraft thermal management systems. Margo and Seyed-Yagoobi (1993) observed increases of up to 71% in forced and free convection heat transfer by utilizing EHD assistance in a convection loop. The intent of the current investigation was to obtain baseline (i.e., without the operational EHD pump) performance data for a EHD-assisted heat pipe in order to accurately quantify the enhancing characteristics of the EHD pump.

Electrohydrodynamic pumping occurs when an electric field interacts with free electric charges in a dielectric fluid. The electric field induces an electromotive force on the free electric charges, dragging the liquid and providing a pumping effect on the liquid medium. This phenomena is illustrated in fig. 1.

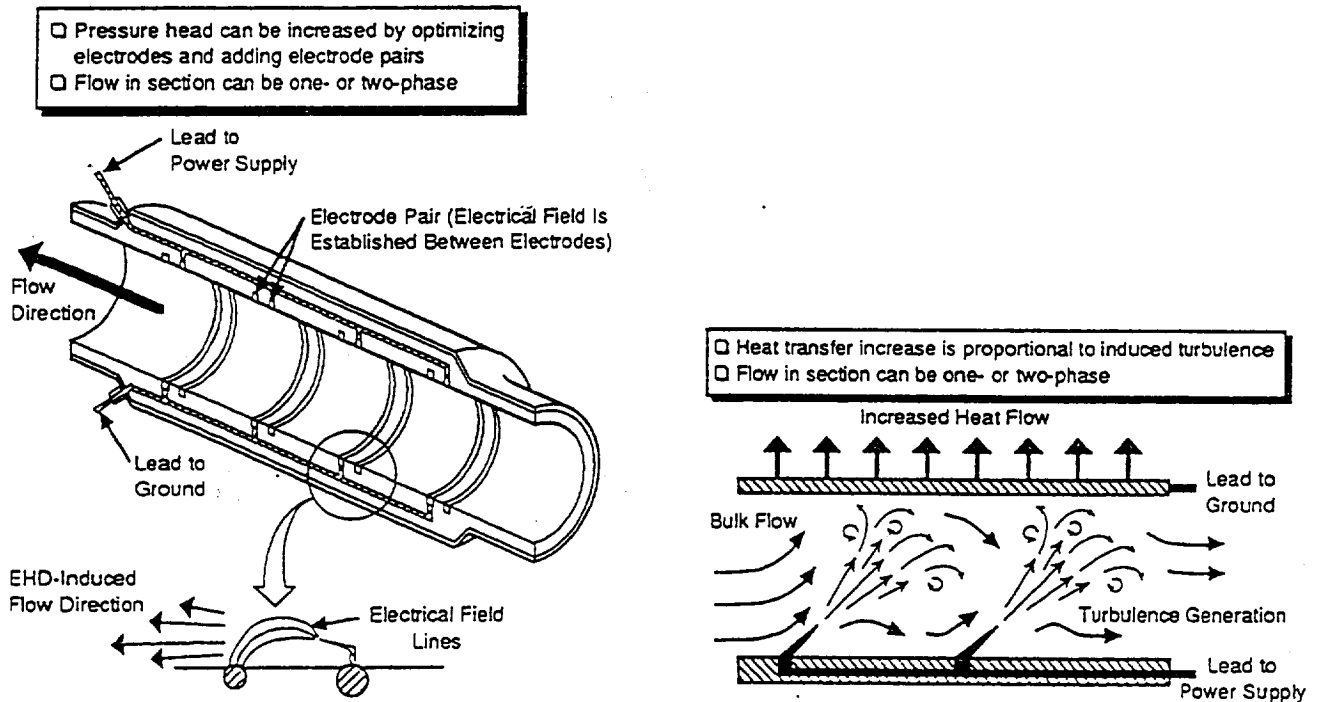


Fig. 1. Principles of the Electrohydrodynamic Pump

EXPERIMENTAL INVESTIGATION

A schematic of this EHD-Assisted Heat Pipe Test Bed utilized in the current investigation is presented in fig. 2. Build-up of the EHD-assisted heat pipe test bed has been completed. As previously stated, the current investigation is intended to obtain baseline performance data for the heat pipe operating without EHD assistance. In order to do this, the maximum heat transport capacity of the unassisted heat pipe will be experimentally determined. Using freon 113 as the heat pipe working fluid, heater power input, condenser temperature, and heat pipe adverse tilt will be varied in order to determine the operating characteristics of the unassisted heat pipe. This will be accomplished by measuring the temperature profiles of both the liquid and vapor flow channels during steady-state operation. A test matrix for this procedure is illustrated in Table 1. Upon completion of this portion of the experimental investigation, data will be compiled and presented in an orderly fashion for further analysis.

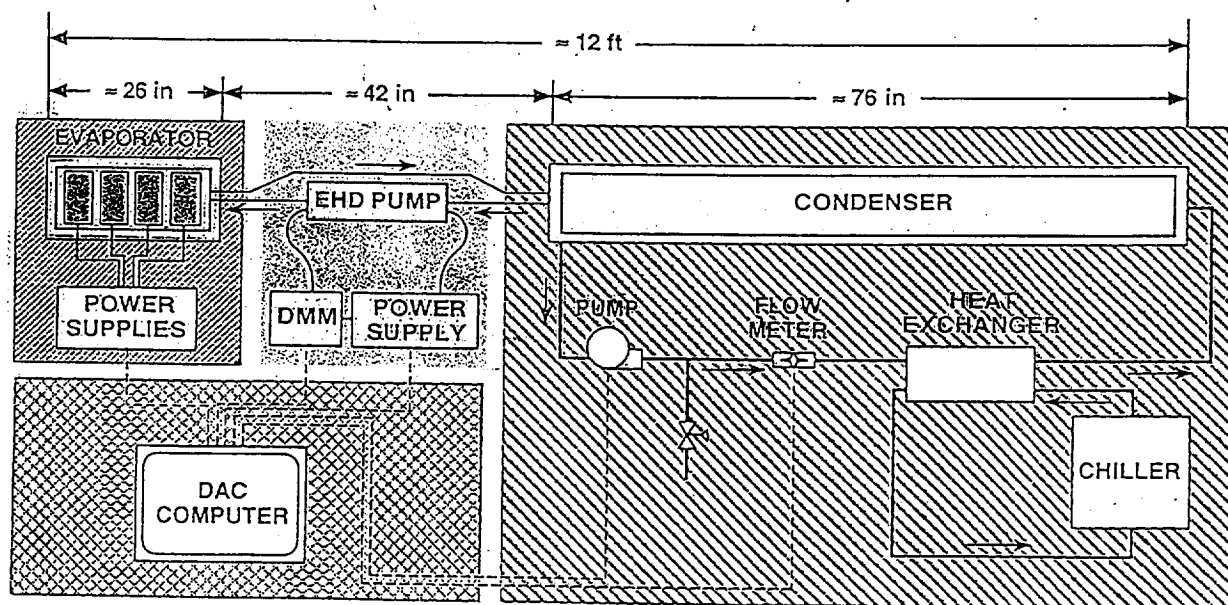


Fig. 2 EHD-Assisted Heat Pipe Schematic

Test Point	Test Stand Inclination (Deg)	Total Power (W)	Evaluation parameter
1	0 to 3.60°, 0.36° increments	100	RTD 21 to 44, TC 45 - 50
2	0 to 3.60°, 0.36° increments	200	RTD 21 to 44, TC 45 - 50
3	0 to 3.60°, 0.36° increments	300	RTD 21 to 44, TC 45 - 50
4	0 to 3.60°, 0.36° increments	400	RTD 21 to 44, TC 45 - 50
5	0 to 3.60°, 0.36° increments	500	RTD 21 to 44, TC 45 - 50
6	0 to 3.60°, 0.36° increments	600	RTD 21 to 44, TC 45 - 50
7	0 to 3.60°, 0.36° increments	700	RTD 21 to 44, TC 45 - 50
8	0 to 3.60°, 0.36° increments	800	RTD 21 to 44, TC 45 - 50
9	0 to 3.60°, 0.36° increments	900	RTD 21 to 44, TC 45 - 50
10	0 to 3.60°, 0.36° increments	1000	RTD 21 to 44, TC 45 - 50
11	0 to 3.60°, 0.36° increments	1100	RTD 21 to 44, TC 45 - 50
12	0 to 3.60°, 0.36° increments	1200	RTD 21 to 44, TC 45 - 50
13	0 to 3.60°, 0.36° increments	1300	RTD 21 to 44, TC 45 - 50
14	0 to 3.60°, 0.36° increments	1400	RTD 21 to 44, TC 45 - 50
15	0 to 3.60°, 0.36° increments	1500	RTD 21 to 44, TC 45 - 50
16	0 to 3.60°, 0.36° increments	1600	RTD 21 to 44, TC 45 - 50

Table 1. Experimental Investigation Test Matrix

ANALYTICAL INVESTIGATION

An analysis of the EHD-assisted heat pipe was performed in order to predict the baseline performance characteristics. Using classical closed-form heat pipe analysis (Chi, 1976), the performance limitations of the freon-charged heat pipe were calculated.

Generally, there are five possible performance limitations for an operating heat pipe. The "sonic" limit is characterized by choked vapor flow in the heat pipe. The boiling limit occurs when nucleate boiling in the heat pipe evaporator, produced from high heat flux levels, creates an unstable region which may not be sufficiently wetted, leading to dry-out. The entrainment limit occurs when the counterflowing liquid and vapor produce a "tearing off" of liquid, also leading to evaporator dry-out. The viscous limit occurs when the vapor pressure of the working fluid is not great enough to drive vapor flow, a limit often associated with low temperature heat pipes. The capillary limit is that limit which occurs when the available capillary pumping pressure in the liquid phase is not great enough to overcome the other pressure drops associated with heat pipe operation such as the pressure drop in the liquid and vapor flow paths and the hydrostatic pressure drop.

An analysis of the operating limits of the Grumman Monogroove heat pipe used in the EHD-assisted heat pipe test bed has indicated that the primary performance limit associated with the test bed is the capillary limit. An analysis of the capillary limit of the EHD-assisted heat pipe test bed, similar to that performed by Ochterbeck and Peterson (1990) has been carried out in the current investigation.

Development of the Analytical Model

The capillary limitation of the Grumman Monogroove heat pipe may be defined by two separate pressure balance statements. First, since the driving pressure difference for return of the liquid to the evaporator is defined by the liquid/vapor interface in the evaporator, the pressure drop across this interface must be equal to the sum of the pressure drops on a path taken from this evaporative interface to the point of liquid replenishment in the evaporator. This may be stated mathematically as follows:

$$\Delta P_{wallcapillary} = \Delta P_{vapor} + \Delta P_{liquid} + \Delta P_{wallwick} + \Delta P_{tilt} + \Delta P_{headdia}$$

In addition to this requirement, the height of the liquid in the axial groove of the heat pipe must be sufficient to continuously supply the wall wicks with liquid. In other words, the liquid height in the axial groove must be great enough to replenish the leading edge of the wall wicks. This may be expressed:

$$\Delta P_{groove, capillary} > \Delta P_{vapor} + \Delta P_{liquid} + \Delta P_{tilt}$$

Each of the terms in the two pressure balance statements may be determined through analysis of the test bed heat pipe.

The pressure drop across the wall capillary in the heat pipe evaporator may be determined from the equation of Young and Laplace (Adamson, 1990).

$$\Delta P_{wall, capillary} = \frac{2\sigma \cos(\theta + \alpha_w)}{W_w}$$

where θ is the wetting angle of the fluid, α_w is the groove taper angle, and W_w is the wall wick width at the height of the meniscus. The pressure drop across the groove meniscus is:

$$\Delta P_{groove, capillary} = \frac{2\sigma \cos(\theta + \alpha_g)}{W_g}$$

The hydrostatic pressure drop associated with the heat pipe orientation may be stated as

$$\Delta P_{ult} = \rho_{liquid}gh.$$

ρ_{liquid} represents liquid density while g is the acceleration due to gravity and h is the adverse tilt of the heat pipe.

The pressure drop associated with flow of the liquid phase may be approximated by considering it as steady-state incompressible pipe flow. As shown in Chi (1976)

$$\Delta P_{liquid} = \frac{2(f Re)\mu_l Q L_{eff}}{\rho_l H_{fg} A_l D_l^2}$$

where L_{eff} is the effective length of the heat pipe, f is the Fanning friction factor associated with the flow, Re is the Reynolds' number, Q is the transported heat, A_l is the area of the liquid flow path, D_l is the hydraulic diameter of the liquid flow path, and H_{fg} is the latent heat of vaporization of the working fluid. A similar expression has been derived for the vapor flow (Chi, 1976).

In the wall-wick structure, similar assumptions were used to calculate the pressure drop term. The wall wick pressure drop may be calculated as

$$\Delta P_{wallwick} = \frac{32\mu_l \pi D_v Q}{8\rho_l H_{fg}} \left[\frac{1}{(nA_w D_w^2 L)_{evap}} + \frac{1}{(nA_w D_w^2 L)_{cond}} \right]$$

where n is the number of grooves per unit length.

Utilization of the individual pressure drop terms into the governing capillary limit equations allows for the determination of the maximum heat transport capacity. The following assumptions were used in developing the computer model which is presented in Appendix A.

- i) The heat pipe operated isothermally, allowing for the calculation of fluid properties at one temperature.
- ii) Vapor flow was incompressible (verified by checking the Mach number).
- iii) The heat pipe was optimally charged.
- iv) The freon fully wet the aluminum surface.
- v) The evaporation and condensation of the freon was uniform across the surfaces of the evaporator and condenser.

Results of the Analytical Model

The maximum heat transport capacity as a function of temperature of the heat pipe is illustrated in fig. 3. As indicated in fig. 3, a maximum heat transport value of 420 Watts is predicted at an adiabatic operating temperature of 125 °C. Fig. 4 illustrates the affects of adverse tilt on the performance limit of the heat pipe test bed. At the optimal operating temperature, maximum heat transport capacity is expected to decrease from 420 W to nearly 55 W as the condenser height is increased from 0 mm to 50 mm.

These predictions seem quite reasonable when compared with other analytical models of the Grumman Monogroove heat pipe (Ochterbeck and Peterson, 1990). The results indicate that the available power to the evaporator of the EHD-assisted heat pipe test bed will be quite adequate (1600 W), as will be the adverse tilt height capability (250 mm).

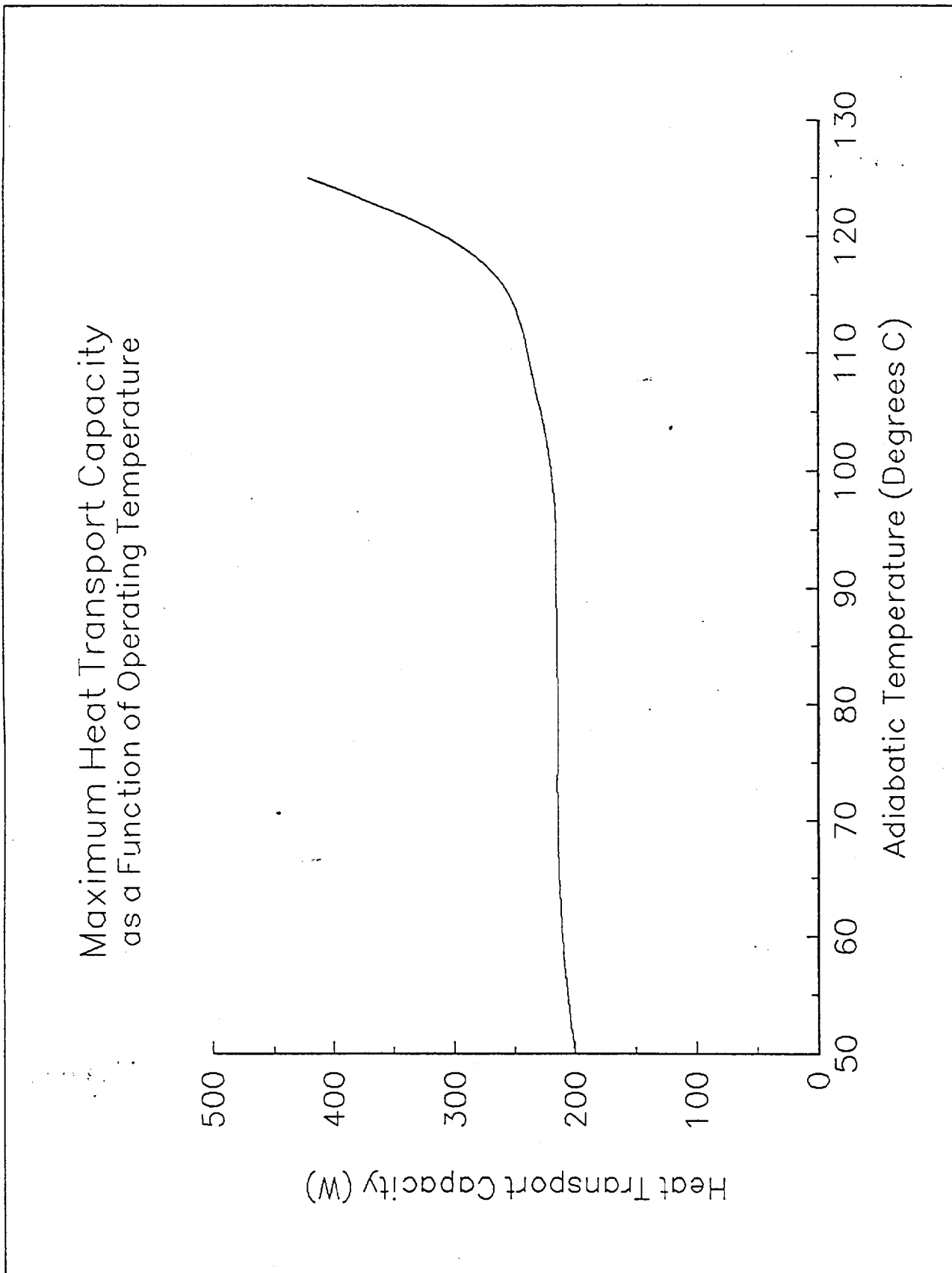


Fig. 3 Maximum Heat Transport Capacity as a Function
of Operating Temperature

Maximum Heat Transport Capacity (1.25 Degrees C)
as a Function of Adverse Tilt

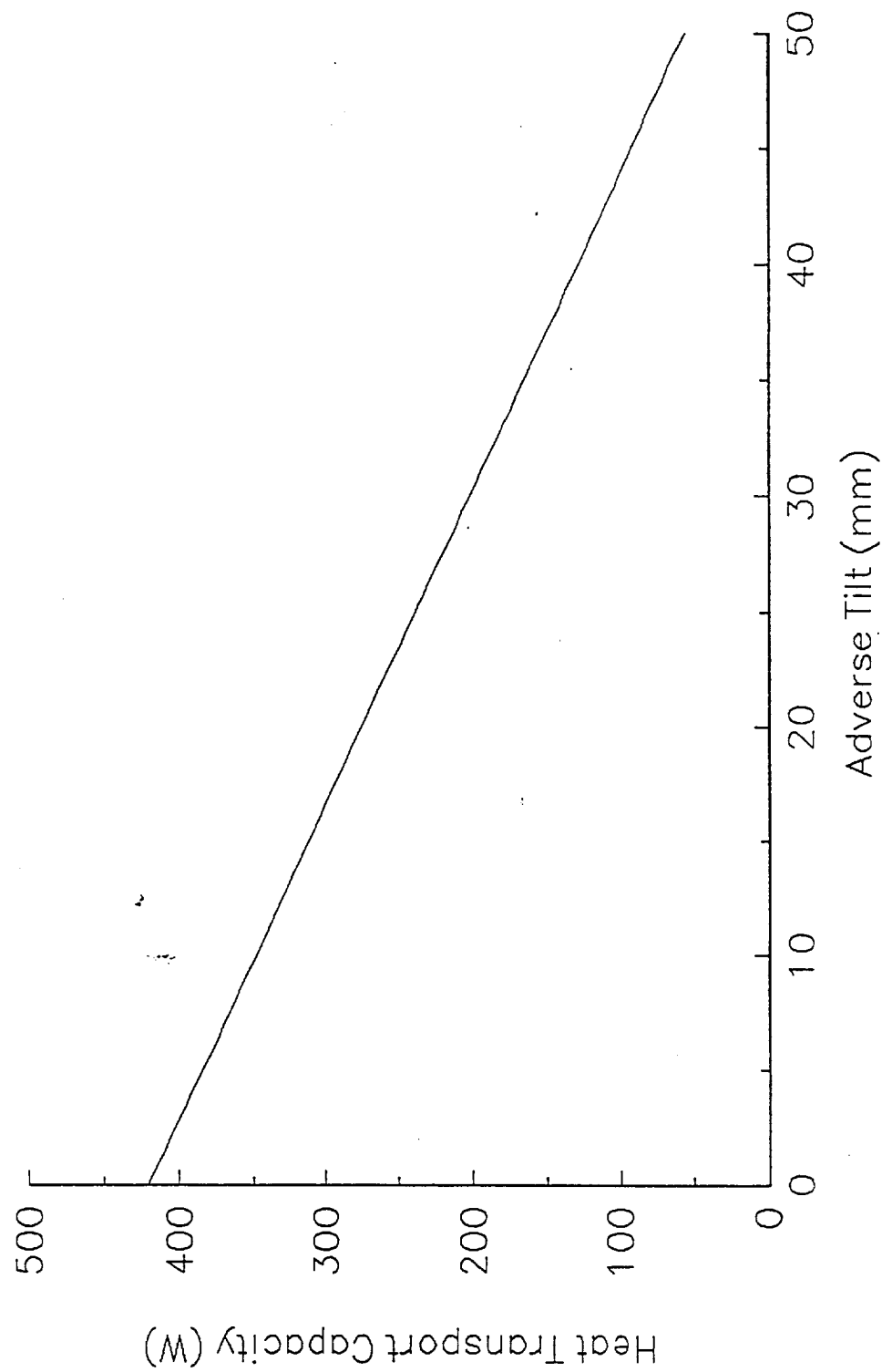


Fig. 4 Maximum Heat Transport Capacity as a Function of Adverse Tilt

CONCLUSIONS

The EHD-Assisted Heat Pipe Test Bed has been successfully fabricated and is ready for comprehensive experimental evaluation. An analytical model of the unassisted heat pipe has been developed which suggests that the capabilities of the experimental facility are well within those which will be required for evaluation. The analytical model has predicted that the maximum heat transport capacity of the heat pipe will be capillary limited and will be approximately equal to 420 W. Additionally, the affects of adverse tilt on the heat transport capacity of the unassisted heat pipe have been modeled. Results suggest that the maximum heat transport capacity of the unassisted heat pipe will decrease by more than 80% at an adverse tilt of 50 mm.

The experimental data to be obtained from the unassisted heat pipe will provide accurate insight into the performance characteristics of the heat pipe. These experimental results should be compared with the results of the modeling effort and an attempt should be made to account for any significant discrepancies. The combined results of the analytical and experimental investigations should lay a solid foundation for evaluation of the heat pipe utilizing EHD assistance.

REFERENCES

Adamson, A. W., 1990, *Physical Chemistry of Surfaces*, 5th Edition, John Wiley and Sons Publishing, New York, NY.

Chi, S. W., 1976, *Heat Pipe Theory and Practice*, McGraw-Hill Book Company, New York, NY.

Margo, B. D., and Seyed-Yagobbi, J., 1993, "Heat Transfer Enhancement Under Various Orientations Resulting From Attractive Mode Induction Electrohydrodynamic Pumping," American Society of Mechanical Engineers, HTD-Vol. 248, Symposium on Fundamentals of Heat Transfer in Electromagnetic, Electrostatic, and Acoustic Fields.

Ochterbeck, J., and Peterson, G. P., "Development of a Generalized Analytical Model for High Capacity External Artery Heat Pipes," Final Report , Submitted to McDonnell Douglas Space Systems Division, Houston, TX 77058, Contract # A96D-J714-STN-KHA-903296.

APPENDIX A
ANALYTICAL MODEL
FORTRAN PROGRAM

program properties

This program is intended for use in the EHD Heat Pipe Investigation
Freon 113 is used in a modified Grumman monogroove heat pipe
Authors: Edouard Motte and Allen Duncan

Variable Definitions:

DPWC = delta p wall capillary
DPMC - delta p monogroove capillary
T - Temperature, degrees C
Vrho - vapor density, kg/m**3
Lrho - liquid density, kg/m**3
Hfg - Latent heat of vaporization, kJ/kg
sig - surface tension, N/m
Cp - vapor specific heat, kJ/kg*k
muv - vapor viscosity, microPascals*s
mul - liquid viscosity, micropascals*s
Kl - liquid thermal conductivity, W/mK
M - molecular weight, kg/kmol
Real T, Vrho, Lrho, Hfg, sig, Cp, muv, mul, Kl, M
Real DPWC, DPMC, DPT, DPL, DPV, Le, Lc, La, Lover, Leff
Real h, Dv, Dl, Q
Real fRel, fRev, Rev
Le = 0.635
Lc = 1.854
La = 0.889
Lover = 3.378
Dv = 15.24e-3
Dl = 10.16e-3
write(*,*)'input h'
read(*,*)h
fRel = 16.
fRev = 16.
open (unit = 4, file = 'output.dat', status = 'unknown')
M = 187.38
Write(*,*)'Input Temperature (C)'
read(*,*)T
T= 125.
write(4,*)'T= ', T
Leff = (Le + Lc)/2. + La
write(4,*)'Leff',Leff
c Subroutine Lden calculates liquid density
Call Lden(T,Lrho)
c Subroutine Vden calculates vapor density (saturation conditions?)
Call Vden(T, Vrho)
write(4,*)'out of vden', T, Vrho
c Subrouting Latent calculates the heat of vaporization
Call Latent(T,Hfg)
c Subroutine Sigma calculates liquid surface tension
Call Sigma(T, sig)
c Subroutine SpecificHeat calculates the vapor specific heat
Call SpecificHeat(T,Cp)
c Subroutine muvapor calculates the viscosity of the vapor
Call muvapor(T,muv)
c Subroutine muliquid calculates the viscosity of the liquid
Call muliquid(T, mul)
c Subroutine Kliquid calculates the thermal conductivity of the liquid
Call Kliquid(T,Kl)
write(4,*)'T = ', T
write(4,*)'Liquid density (kg/m**3)= ', Lrho
write(4,*)'vapor density (kg/m**#)= ', Vrho

```

write(4,*)'Heat of Vaporization (kj/kg) = ', Hfg
write(4,*)'surface tension (N/m)', sig
write(4,*)'Vapor specific heat (kj/kg*k)', Cp
write(4,*)'Vapor viscosity (Pa*s)', muv
write(4,*)'Liquid viscosity (Pa*s)', mul
write(4,*)'Liquid thermal conductivity (W/mK)', Kl
c Subroutine DPwallCap calculates the pressure drop across the liquid
c vapor interface of the wall and monogroove capillaries
  Call DPwallCap(sig, DPWC, DPMC)
  write(4,*)'delta p capillary (Pa)', DPWC
  write(4,*)'delta p monogroove (Pa)', DPMC
c Subroutine DPtilt calculates the pressure drop due to adverse tilt
  call DPtilt(Lrho, h, DPT)
  write(4,*)'Lrho', Lrho
  write(4,*)'h', h
  write(4,*)'DPT', DPT
c Subroutine DPhydro represents the hydrostatic loss associated with the wall
c groove flow
  call DPhydro(Lrho, Dv, DPH)
  write(4,*)'DPH', DPH
c Subroutine Dpliq calculates the pressure drop in the laminar liquid flow
c channel
  Call Dpliq(fRel, mul, Lrho, Leff, Hfg, Dl, DPL)
c subroutine Dpvap calculates the pressure drop associated with the vapor flow
  call Dpvap(fRev,muv, Leff, Vrho, Hfg, Dv,DPV)
c subroutine Heat calculates the heat transport capacity
  call Heat(DPWC, DPMC, DPT, DPH, DPV, DPL, Q)
  call Reynolds(Vrho, Q, Dv, Hfg, muv, Rev)\
  write(*,*)'Q = ', Q
  If(Rev.gt.2300.) Call TurbHeat(DPWC, DPMC, DPT, DPH, DPL,
*   Q, Leff, Rev,Dv,Vrho, Hfg)
  stop
end
Subroutine Lden (T,Lrho)
Real T, Lrho
Lrho = 1619.662 - (2.607 * T) - (0.0021 * (T**2))
return
end
Subroutine Vden(T, Vrho)
Real T, Vrho
Vrho = 1.2296 + (0.05363 * T) + (0.0010399 * T**2.) +
% 1.21529e-5*(T**3.)
return
end
Subroutine Latent(T, Hfg)
Real T, Hfg
Hfg = 158.0593 - 0.2675*T - 0.0006 * (T**2)
return
end
Subroutine sigma (T, sig)
real T, sig
sig = 0.0188 - 0.0001 * T
return
end
Subroutine SpecificHeat(T,Cp)
Real T, Cp
Cp = 0.6170 + 0.0010 * T
return
end
Subroutine muvapor(T,muv)
real T, muv
muv = 8.2651 + (0.0635*T) - 0.0002 * (T ** 2)
muv = muv *1.e-6
return
end
Subroutine muliquid(T, mul)

```

```

      real T, mul
      mul = 990.6387 - 16.7189*T + 0.1862*(T**2) - 0.0009*(T**3)
      mul = mul*1.e-6
      return
    end
    Subroutine Kliquid(T,Kl)
      real T, Kl
      Kl = 0.0801 - 0.0002*T
      return
    end
    Subroutine DPWallCap(sig, DPWC, DPMC)
      Real sig, DPWC, DPMC, theta, alphaW, Wwe, Wwc, Wm
      Real Rwe, Rwc, Depth
      theta = 0.
c   alphaW is the taper angle
c   Wall wick widths at the height of the meniscus
c   evaporator and condenser, respectively
c   Wwe represents the wall wick depth at the height of the meniscus, evaporator
      Wwe = 0.014e-3
c   Wwc - wall wick width, height of meniscus, condenser
      Wwc = 0.165e-3
c   Rwe - wall wick root width, evaporator
      Rwe = 0.014e-3
c   Rwc - wall wick root width, condenser
      Rwc = 0.089e-3
c   Depth - depth of the wall wick grooves
      Depth = 0.196e-3
c   WM = monogroove width
      WM = 0.25e-3
      alphaW = Atan((Wwe - Rwe)/(2*Depth))
      write(4,*) 'alphaW (rad)', alphaW
      write(4,*) 'Wwe', Wwe
      write(4,*) 'theta (rad)', theta
      write(4,*) 'sigma (N/m)', sig
      write(4,*) 'cos(theta + alphaW)', cos(theta + alphaW)
      DPWC = ((2*sig*cos(theta + alphaW))/Wwe)
      DPMC = 2.*sig*cos(theta)/WM
      return
    end
    Subroutine DPtilt(Lrho, h, DPT)
      real Lrho, h, DPT, g
      g = 9.81
      DPT = (Lrho*g*h)
      return
    end
    subroutine DPhydro(Lrho, Dv, DPH)
      real Lrho, Dv, DPH, g
      g = 9.81
      write(4,*) 'hydro', Lrho, Dv, g
      DPH = Lrho*g*Dv
      return
    end
    subroutine DPlig(fRel, mul, Lrho, Leff, hfg, Dl, DPL)
      real fRel, mul, Lrho, Leff, hfg, Dl, DPL
      DPL = (2.*fRel*mul*Leff)/(Lrho*Hfg*3.14159*(Dl**4.))
      write(4,*) 'frel', fRel
      write(4,*) 'mul', mul
      write(4,*) 'Lrho', Lrho
      write(4,*) 'leff', Leff
      write(4,*) 'hfg', hfg
      write(4,*) 'Dl', Dl
      write(4,*) 'DPL', DPL
      return
    end
    Subroutine Dpvap(fRev, muv, Leff, Vrho, Hfg, Dv, DPV)
      Real fRev, muv, Leff, Vrho, Hfg, Dv, DPV

```

```

write(4,*)'fRev',fRev,'muv',muv,'Leff', Leff,'Vrho', Vrho
write(4,*)'Hfg', Hfg,'Dv',Dv
DPV = 2.*fRev*muv*Leff/(Vrho*3.14159*Hfg*(Dv**4.))
write(4,*)'dpv',DPV
return
end
Subroutine Heat(DPWC, DPMC, DPT, DPH, DPV, DPL, Q)
Real DPWC, DPMC, DPT, DPH, DPV, DPL, Q
Q = (DPWC-DPT-DPH)/(DPV+DPL)
write(4,*)'Q=', Q
return
end
Subroutine Reynolds(Vrho, Q, Dv, Hfg, muv, Rev)
Real Vrho, Q, Dv, Hfg, muv, Rev
Rev = (Vrho*Q*Dv)/(Hfg*muv)
write(4,*)'vapor reynolds no', Rev
return
end
Subroutine TurbHeat(DPWC, DPMC, DPT, DPH, DPL, Q,
* Leff, Rev,Dv, Vrho, Hfg)
Real DPWC, DPMC, DPT, DPH, DPL, Q, DPVT, F, Leff, Rev
Real A, B, C, Q1, Q2, Hfg, D, E
write(4,*)'DPWC', DPWC, 'DPMC', DPMC, 'DPT', DPT, 'DPH', DPH
write(4,*)'DPL',DPL,'Q',Q, 'Leff', Leff, 'Rev', Rev
write(4,*)'Dv', Dv, 'Vrho', Vrho, 'Hfg', Hfg
F = 2./((2.236*(LOG(Rev))-4.639)**2.)
write(4,*)'fturb',F
D = 8.*F*Leff
E= Vrho*(Hfg**2.)*(3.14159**2.)*(Dv**6.)/16.
DPVT = D/E
A = DPVT
B = DPL
C = -1.*(DPWC-DPT-DPH)
write(4,*)'a',a,'b',b,'c',c
Q1 = ((-1.*B) +SQRT((B**2.)-(4.*A*C))) /(2.*A)
Q2 = ((-1.*B) -SQRT((B**2.)-(4.*A*C))) /(2.*A)
write(4,*)'Q1', Q1
write(4,*)'Q2', Q2
return
end

```